JOURNAL OF BACTERIOLOGY, Feb. 2003, p. 779–787 Vol. 185, No. 3
0021-9193/03/$08.00+0 DOI: 10.1128/JB.185.3.779–787.2003

Sizing the Holin Lesion with an Endolysin–β-Galactosidase Fusion

Ing-Nang Wang,† John Deaton, and Ry Young*

Department of Biochemistry and Biophysics, Texas A&M University, College Station, Texas 77843-2128

Received 16 July 2002/Accepted 4 November 2002

Double-stranded DNA phages require two proteins for efficient host lysis: the endolysin, a muralytic enzyme, and the holin, a small membrane protein. In an event that defines the end of the vegetative cycle, the λ holin S acts suddenly to permeabilize the membrane. This permeabilization enables the R endolysin to attack the cell wall, after which cell lysis occurs within seconds. A C-terminal fusion of the R endolysin with full-length β-galactosidase (β-Gal) was tested for lytic competence in the context of the late-gene expression system of an induced λ lysogen. Under these conditions, the hybrid R–β-Gal product, an active tetrameric β-Gal greater than 480 kDa in mass, was fully functional in lysis mediated by the S holin. Western blot analysis demonstrated that the lytic competence was not due to the proteolytic release of the endolysin domain of the R–β-Gal fusion protein. The ability of this massive complex to be released by the S holin suggests that S causes a generalized membrane disruption rather than a regular oligomeric membrane pore. Similar results were obtained with an early lysis variant of the S holin and also in parallel experiments with the T4 holin, T, in an identical lambda context. However, premature holin lesions triggered by depolarization of the membrane were nonpermissive for the hybrid endolysin, indicating that these premature lesions constituted less-profound damage to the membrane. Finally, a truncated T holin functional in lysis with the endolysin is completely incompetent for lysis with the hybrid endolysin. A model for the formation of the membrane lesion within homo-oligomeric rafts of holin proteins is discussed.

Double-stranded DNA (dsDNA) phages use a holin-endolysin strategy to achieve a scheduled, efficient host lysis (27, 31). The endolysin is an enzyme with one or more muralytic activities against the glycosidic, amide, or peptide bonds of the peptidoglycan. Holins are small membrane proteins with unparalleled diversity, constituting at least three topological classes (classes I, II, and III, with three, two, and one transmembrane domain [TMD], respectively) and at least 34 unrelated protein families (27). Holin and endolysin genes can be identified by analysis of the genomic sequences of most dsDNA phages, although only a few have been characterized in terms of in vivo function. For phages tested to date, the endolysin requires the holin to achieve access to the peptidoglycan, except in some phages of gram-positive bacteria, where the endolysins use the *sec* system (20). The best-characterized example of holin-endolysin systems is that of phage λ, where the *S* gene encodes the holin and *R* encodes the endolysin, a transglycosylase. The vegetative cycle of an induced λS^+ lysogen is terminated abruptly by host lysis at 50 min in almost all cells in the culture, whereas in λ*S*am inductions, intracellular accumulation of completed virions and R endolysin activity continue indefinitely. The remarkably precise timing of holin function is not understood. Somehow, membrane integrity, at least as reflected by the level of the proton motive force, is maintained until the holin is triggered a few seconds before lysis. *S* missense alleles that encode stable protein products with triggering times ranging from 19 to more than 120 min after lysogenic induction are known (27).

Nothing is known of the structure of the membrane lesion. It appears to be a homo-oligomer of S (8). Purified S protein has been shown to permeabilize liposomes in vitro (25). Four different enzymatic activities of endolysins have been found: glycosidase (e.g., T4 gp*e* lysozyme and P22 gp*19* lysozyme), transglycosylase (e.g., λ R lysozyme and P2 K), amidase (e.g., T7 gp*3.5* lysozyme and φ11 murein hydrolase), and endopeptidase (e.g., φ11 murein hydrolase). To date, every heterologous endolysin tested has been found to support lysis as long as the S holin function is provided, indicating that there is no required specific interaction between the holin and endolysin. The absence of specific interactions implies a large, nonspecific lesion in the membrane. Despite this, no ultrastructural evidence has been obtained for membrane pores (27).

In the crystal structure of lambda lysozyme R, the C terminus appears to be free for appending fusion domains (6). This suggests that the size of the holin lesion can be probed by fusing a series of large protein domains to the C terminus of the endolysin. The results of such a study are reported here and discussed in terms of a general model for the membrane lesion formed by holins.

MATERIALS AND METHODS

Bacterial strains, bacteriophages, plasmids, primers, enzyme assays, and culture growth. The bacterial strains MC4100 and CQ21 and the lysis-defective thermoinducible prophage λ*kan*Δ(*SR*) have been described previously (16, 26). The plasmids and primers used in this study are listed in Table 1. All bacterial cultures were grown in standard Luria-Bertani medium, supplemented with various antibiotics when appropriate. The concentrations for the supplements were as follows: 100 μg/ml for ampicillin and chloramphenicol, 10 μg/ml for kanamycin, and 10 μg/ml for tetracycline. In addition, X-Gal (5-bromo-4-chloro-3-indolyl-β-D-galactopyranoside; Sigma) was used at 40 μg/ml in top agar for detecting β-galactosidase (β-Gal) activity in plaques. When required for induction, isopropyl β-D-thiogalactopyranoside (IPTG) was added to liquid cultures at a final concentration of 1 mM. β-Gal assays were performed according to the method of Miller (14). Conversion of Miller units to international units and then

* Corresponding author. Mailing address: Department of Biochemistry and Biophysics, 2128 TAMU, Texas A&M University, College Station, TX 77843-2128. Phone: (979) 845-2087. Fax: (979) 862-4718. E-mail: ryland@tamu.edu.

† Present address: Department of Biological Sciences, State University of New York, Albany, NY 12222.

TABLE 1. Plasmids and primers used in this study

	Relevant feature or sequence (5′ to 3′)[a]	Source
Plasmids		
pS105R$^-$	*S105* under pR′ control, *RRzRzl* deleted, pBR322 replicon	7
pS105A52GR$^-$	A52G allele isogenic to pS105R$^-$	7
pT4-tR$^-$	T4 *t* under pR′ control; isogenic to pS105R$^-$	17
pER-TΔ69	T4 *t* under pR′ control; isogenic to pS105R$^-$	This work
pT4-tΔ69	T4 *t* under pR′ control; last 69 residues of T are deleted	E. Ramanculov, unpublished data
pS105mycR	*S105 RRzRzl* lysis cassette encoding *c-myc*-tagged R (Fig. 1)	This work
pS105mycRϕlacZ	pS105mycR with *lacZ* reading frame inserted at end of the *R* sequence (Fig. 1)	This work
pZA32-luc	IPTG-inducible luciferase gene, p15A replicon	12
pZA32-mycR	*mycR* replacement of *luc* in pZA32-luc	This work
pZA32-mycRϕlacZ	*mycRϕlacZ* replacement of *luc* in pZA32-luc	This work
pZS*32-luc	pSC101* replicon, isogenic to pZA32-luc	This work
pZS*32-mycR	pSC101* replicon, isogenic to pZA32-mycR	This work
Primers		
mycRFor	AGTTACTCTTCTATTAGCGAAGAAGATCTGGTAGAAATCAATAAT	
mycRRev	AGTTACTCTTCGAATCAGTTTCTGTTCCATCTTCTACTCCGG	
lacZI4For	AGTTACTCTTCAGATATTACGGATTCACTGGCC	
lacZK1024Rev	AGTTACTCTTCGTACTTTTTGACACCAGACCAA	
RV158For	AGTTACTCTTCAGTATGAGCAGAGTCACCGCGA	
RD157Rev	AGTTACTCTTCGATCAATCTCTCTGACCGTTCC	
KpnIRFor	CCGGAGGGTACCATGGAACAGAAACTGATT	
XbaIRRev	GATAATTCTAGAGACTCTGCTCATACATCA	
HindQFor	ACCGCATTAAAGCTTGAAGG	
RBamRev	GGTTTTCTGGGATCCGTTAT	

[a] The sequences encoding the c-*myc* epitope are underlined in the first two entries. In the last four entries, a unique restriction site is underlined.

to enzyme molecules was done by assuming 1,000 IU per mg of β-Gal, which corresponds to the maximum grade of purified enzyme (Sigma) and a millimolar extinction coefficient of 4.5 at 420 nm for *o*-nitrophenol under the assay conditions (15).

Growth media and culture monitoring. Cultures were grown in Luria-Bertani medium, supplemented with appropriate antibiotics. Induction of lysogens and plasmid-borne lysis genes and monitoring of the induced cultures under strictly controlled conditions have been described previously (4, 25).

Standard DNA manipulation, PCR, and DNA sequencing. Standard DNA manipulation, PCR, and DNA sequencing have been described previously (7, 24, 26). The following conditions were used for all PCR amplifications, which were done with *Pfu* DNA polymerase (Stratagene, La Jolla, Calif.): one cycle of 94°C for 1 min, followed by 15 cycles of 94°C for 30 s, 53°C for 30 s, and 72°C for several minutes, with 2 min being used for every 1-kb extension.

c-*myc* tagging of λ R. To detect the presence of the λ R protein, the N terminus of the endolysin was tagged with the c-*myc* epitope (Fig. 1) by a modified method of "seamless cloning" (Stratagene) (25). Briefly, instead of separately PCR amplifying the desired insert and the cloning vector and joining both together, as described for the original protocol, the DNA sequence encoding the c-*myc* epitope sequence (EQKLISEEDL) was broken into two parts and included in the design of the primers mycRFor and mycRRev (Table 1). As a result, the c-*myc* epitope was inserted between the first and second amino acid residues of λ R (Fig. 1), encoded by the product plasmid pS105mycR. The template for the epitope tagging was plasmid pS105, a pBR322 derivative containing the λ lysis cassette *S105RRzRz1* (25). The *S105* allele of *S*, with the start codon of the antiholin reading frame inactivated, produces only the holin S105 and was chosen to simplify the interpretation of the lysis kinetics because it exhibits all of the lysis timing and triggering properties of the parental *S* allele, except that the onset of lysis is slightly accelerated (3). The insertion of the epitope-encoding sequence in *R* alters the 3′ end of the partially overlapping *S* cistron, changing the C-terminal cytoplasmic domain of the S holin to a more acidic sequence (Fig. 1). The cytoplasmic C terminus has been shown to be dispensable for lysis, although the overall charge of this domain does affect lysis timing (2, 19).

Construction of pS105mycRϕlacZ and recombinant phage. The λ *R* gene was fused with *E. coli lacZ* by the seamless cloning protocol (Stratagene). Briefly, the *lacZ* gene was PCR amplified with the primers lacZI4For and lacZK1024Rev

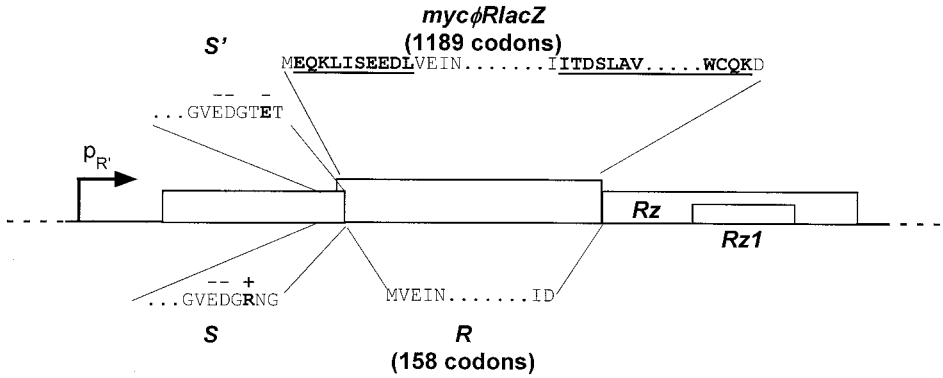

FIG. 1. Modification of *R* with c-*myc* and *lacZ* at the 5′ and 3′ termini. Shown are the predicted alterations at the termini of the S and R proteins deriving from the insertions described in the text, in the context of the promoter-proximal region of the λ late transcriptional unit *SRRzRz1*. The *S* allele is *S105*, where the start codon for the S107 antiholin has been eliminated (7). The *S′* allele created by the insertion of the c-*myc* sequence at the start of *R* has 3 C-terminal residues altered, with a predicted net change of −2 in charge. The c-myc (10 residues) and β-Gal (1,021 residues) sequences are shown in underlined boldface as insertions after codon 1 and before codon 158 of *R*, respectively.

(Table 1). Amplification with these primers encompasses the entire *lacZ* sequence except for the first three codons. The plasmid pS105mycR was used as the template for PCR amplification with the primers RV158For and RD157Rev (Table 1). After digestion with *Eam*1104I and ligation of these two PCR products according to the manufacturer's instructions, the resulting plasmid, with *lacZ* inserted between the last and the penultimate codons of *R*, was designated pS105mycRϕlacZ (Fig. 1). Finally, plasmids pS105mycR and pS105mycRϕlacZ were transformed into MC4100 [λ*kan*Δ(*SR*)]. Phages carrying the chimeric endolysin genes were obtained by induction of the transformants and plating of the cell-free lysate on MC4100 for plaque-forming recombinants.

Construction of pZA32-mycR, pZA32-mycRϕlacZ, and pZS*32-mycR. The pZ plasmid series, designed in a modular fashion for ease of swapping replication origins, regulatory elements, and antibiotic resistance genes (12), was used to independently express the *mycR* and *mycRϕlacZ* genes. To modulate the expression level, *mycR* was placed under the control of the chimeric promoter $P_{LlacO-1}$, which consists of the λ P_L promoter and *E. coli lacO* operator sequences. The PCR primer pair *Kpn*IRFor and *Xba*IRRev (Table 1), which contain, respectively, the *Kpn*I and the *Xba*I recognition sequences, was used to PCR amplify the *mycR* sequence from pS105mycR (see above). The PCR product was double digested with *Kpn*I and *Xba*I and cloned into the corresponding sites on pZE12-luc. The resulting plasmid, pZE12-mycR, was double digested with *Kpn*I and *Avr*II to excise the *mycR* fragment (without the regulatory element), which was cloned into the same sites on pZA31-luc to generate pZA31-mycR. Plasmid pZA32-luc was constructed first by double digesting pZE12-luc with *Aat*II and *Avr*II to excise *luc* together with the regulatory element of the promoter $P_{LlacO-1}$. The fragment was cloned into the same sites on pZA31-mycR, resulting in pZA32-luc. To construct pZA32-mycR, pZA31-mycR was first double digested with *Kpn*I and *Avr*II to excise the *mycR* without the regulatory element. The fragment was cloned into the same sites on pZA32-luc, resulting in pZA32-mycR. To construct pZA32-mycRϕlacZ, the primer pairs *Kpn*IRFor and *Xba*IRRev were used to PCR amplify the *mycRϕlacZ* sequence by using pS105mycRϕlacZ as the template. After double digestion with *Kpn*I and *Xba*I, the PCR product, containing the entire *mycRϕlacZ* sequence, was cloned into the same site on pZE12-luc, resulting in pZE12-mycRϕlacZ. After double digestion of pZE12-mycRFlacZ with *Kpn*I and *Avr*II, the fragment containing the *mycRϕlacZ* sequence was cloned into the same site on pZA32-mycR, resulting in pZA32-mycRFlacZ. To further reduce the basal expression level of *mycR*, the *ori* genes of pZA32-luc and pZA32-mycR (from p15A) were swapped with a mutant pSC101 *ori* gene, which supports the production of about three to four copies per cell (12). To construct pZS*32-luc and pZS*32-mycR, an *Avr*II-*Sac*I fragment containing the pSC101* *ori* gene from pZS*24-MCS1 was cloned into the same sites on pZA32-luc and pZA32-mycR, respectively.

Construction of pT4-tR$^-$ plasmids. The plasmid pER-t, carrying the complete T4 *t* holin gene and the λ*RRzRz1* genes (17), was used as the template and was PCR amplified with the primer pair HindQFor (binds at the *Hin*dIII site flanking the λ late promoter) and RBamRev (binds at the *Aat*II site within *R*, containing the *Hin*dIII and *Bam*HI sites) (Table 1). The resulting PCR product, containing the λ pR′ promoter, the entire T4 *t* gene, and a partial λ *R* gene encoding the first 28 residues of the R protein, was doubled digested with *Hin*dIII and the *Bam*HI and cloned into the same sites on pBR322, resulting in pT4-tR$^-$. pER-TΔ69 was constructed by *Aat*II digestion of pER-t and religation. The resulting *tΔ69* deletion allele encodes a T protein with the last 69 residues of its predicted periplasmic domain replaced with the following 27 residues: QVALFGEMCA EPLFVYFSKYIQICIRS.

Protein sample preparation, SDS-PAGE, Western blotting, and chromatography. Total protein in cell lysates was extracted as described previously (29). Previously described procedures were used for sodium dodecyl sulfate-polyacrylamide gel electrophoresis (SDS-PAGE), Western blotting, and immunodetection (7), with exceptions. For SDS-PAGE, the protein samples were resolved on 10% Tris-Tricine gels. For immunodetection of the c-*myc* epitope, the mouse anti-c-*myc* monoclonal antibody (1:1,000 dilution; BabCo, Richmond, Calif.) and the goat anti-mouse immunoglobulin conjugated to horseradish peroxidase (1:1,000 dilution; Pierce, Rockford, Ill.) were used as the primary and secondary antibodies, respectively. Blots were also developed with SuperSignal chemiluminescence (Pierce), according the manufacturer's instructions. Gel filtration analyses were performed on an AKTA (Amersham Pharmacia) workstation. Fresh lysates (15 ml) were chilled on ice, cleared of debris by 10 min of centrifugation at 9,000 rpm in a JA-20 rotor in the cold, filtered through a 0.22-μm-pore-size sterilization filter, and concentrated to 2 ml by centrifugation in an Amicon Centriplus (4 h at 3,100 rpm, according to the manufacturer's instructions). The resulting 2-ml samples were chromatographed with a Superdex 200 HR 10/30 column, collected in 1-ml fractions, and (with Pharmacia high- and low-molecular-weight gel filtration calibration kit markers) dissolved into each sample according to the manufacturer's instructions. As controls, samples and markers were also resolved separately on the column. Selected elution fractions were concentrated and analyzed by Western blotting with anti-c-*myc* antibodies as described above.

RESULTS

Construction of the *mycRϕlacZ* fusion gene: effect on holin timing. The high-resolution structure of the λ R endolysin revealed that both the N and C termini are solvent exposed and available for protein fusions (6). We reasoned that appending a sufficiently large, independent folding domain at the C terminus would create a lysis-defective *R* allele, because the fusion product would be unable to pass through the holin lesion. To test this notion, we fused essentially the entire sequence of the *lacZ* gene after the penultimate codon of *R*, creating an *RϕlacZ* fusion reading frame encoding a polypeptide, R–β-Gal, of more than 1,100 residues. To ensure that we could detect the hybrid protein and assess its integrity, a sequence encoding the c-*myc* epitope was inserted immediately after the start codon of the *R* and the *RϕlacZ* reading frames in the context of the *S105RRzRz1* lysis cassette (Fig. 1). With the *S105mycRRzRz1* cassette, lysis is triggered at about 35 min in the context of the plasmid-borne cassette and at about 45 min in the context of the phage. The results clearly show that the mycR endolysin is fully functional in terms of the saltatory lysis observed after holin triggering (Fig. 2).

Lytic function of the endolysin–β-Gal chimera. The predicted product of the *mycRϕlacZ* gene, mycR–β-Gal, is a polypeptide of 1,189 residues, almost eight times larger than the mycR product (Fig. 1). If folded properly, this product would be even more massive in solution as a result of the tetramerization of the β-Gal domain, creating a tetramer of mycR–β-Gal chimeric endolysins of approximately 500 kDa (10) (see below). Host lysis supported by such a massive endolysin would indicate that whatever the holin-mediated lesion is, it is capable of allowing the membrane transit of a folded protein several times too large even for the channel size of the Tat export system, which, at 5 to 9 nm in diameter, is thought to be the largest known channel in bacterial membranes (30). To test the lytic competency of the *mycRϕlacZ* construct, lysogens of λΔ(*SR*) carrying a plasmid with the isogenic lysis gene cluster *SmycRRzRz1* or *SmycRϕlacZRzRz1* under the control of the late promoter $P_{R'}$ were subjected to induction (Fig. 2A). Both cultures underwent a sudden and quantitative lysis, with the only detectable difference being a somewhat slower onset of the most rapid phase of the loss of turbidity with the mycR–β-Gal chimera. Moreover, levels of premature lysis, initiated by the addition of chloroform before the triggering time, were very similar in cultures carrying the parental endolysin and endolysin–β-Gal fusion alleles. The simplest interpretation is that mycR–β-Gal is not seriously compromised in its access to or activity on its substrate, the peptidoglycan. This demonstrates not only that the chimeric endolysin is functional as a muralytic enzyme but also that it can use the S-mediated "hole" to cross the membrane.

The isogenic *SmycRRzRz1* and *SmycRϕlacZRzRz1* lysis cassettes were recombined onto the phage genome by selecting for plaque-forming progeny from the lysates derived from the inductions described above. Lysogens carrying these recombi-

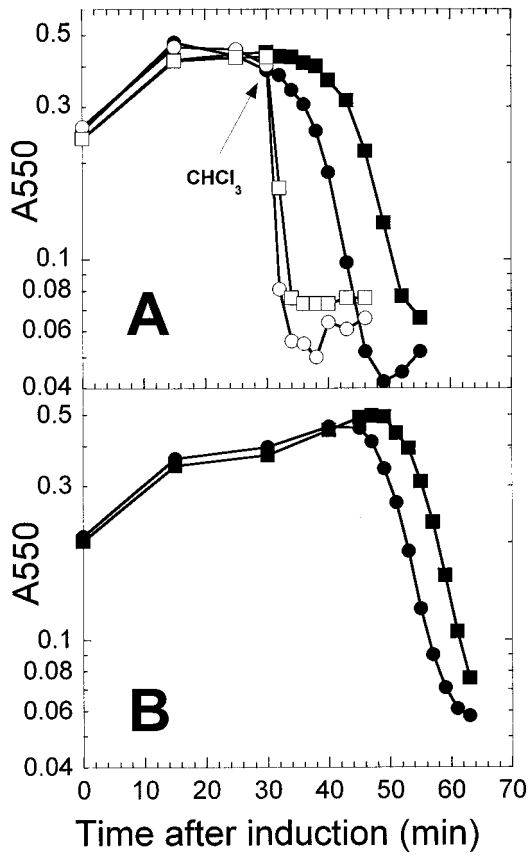

FIG. 2. The endolysin–β-Gal fusion is fully functional in holin-mediated lysis. Culture growth and lysis were monitored by determining the A_{550} after thermal inductions. (A) Induction of λΔ(*SR*) lysogens carrying pS105mycR (circles) or pS105mycRϕlacZ (squares). Open symbols, repeat experiment with approximately 1% $CHCl_3$ added at the indicated time; filled symbols, untreated cultures. (B) Induction of MC4100 lysogens carrying λ*mycR* or λ*mycRϕlacZ* prophages.

nants as prophages were constructed and subjected to standard inductions. Again, the induced λ*mycRϕlacZ* lysogen exhibited sharply defined lysis indistinguishable from that of the isogenic *mycR* lysogen except for a reproducible 5-min delay in the onset of lysis (Fig. 2B). The delay in lysis triggering in both the plasmid and phage contexts suggested that holin accumulation was reduced in the induced λ*mycRϕlacZ* lysogen. Because the antibodies available were raised against a synthetic peptide corresponding to the last 16 residues of the S protein, the alteration of the C-terminal coding sequence of *S* precluded direct assessment of holin accumulation by immunoblotting. However, a delay in holin function without reduction of late gene expression would result in the accumulation of more virions (16). Determining the titers of the induced lysates revealed that the burst size of the λ*mycRϕlacZ* phage was approximately 39, compared to 65 for λ*mycR*, a 40% reduction; the reduced burst size and longer vegetative cycle resulted in smaller plaques (Fig. 3). Evidently, the insertion of the 3-kb *lacZ* sequence into the lysis cassette had a slight but detectable negative effect on the stability or translatability of part or all of the late transcript encoding the holin and all of the morphogenetic proteins of λ, resulting in a marginally lower rate of holin accumulation and thus slightly delayed lysis.

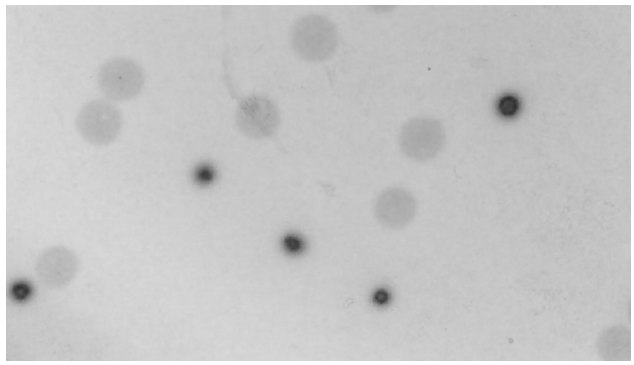

FIG. 3. Plaque-forming ability of λ with the *mycRϕlacZ* hybrid endolysin gene. λ*mycR* and λ*mycRϕlacZ* were mixed at a 1:1 ratio and plated with MC4100 in top agar containing X-Gal.

The *Rϕlac*Z fusion gene product is intact and retains β-Gal function. In principle, the lytic event supported by the *mycRϕlacZ* fusion gene may have been due to a small N-terminal proteolytic fragment retaining the muralytic activity. Immunoblot analysis, however, revealed that the mycR and mycR–β-Gal proteins accumulated to approximately the same level but also that almost all of the hybrid protein retained its full length and even the small amount of proteolytic product retained most of the β-Gal domain (Fig. 4A). Moreover, the presence of an immunologically undetectable amount of an N-terminal proteolytic fragment corresponding to the free mycR muralytic domain could be ruled out because, at levels of mycR endolysin at which the rate of lysis was already limiting (Fig. 4B), no corresponding fragment could be detected in blots of samples containing the chimeric endolysin (Fig. 4C). We conclude that the full-sized hybrid mycR–β-Gal polypeptide is fully functional as an endolysin for λ lysis. (It should be noted that a small reduction in lysis gene expression, which has been suggested to underlie the slight delay in lysis and reduced burst size of the λ*cmycRϕlacZ* phage, would not be detectable in these immunoblotting experiments.)

If the mycR–β-Gal fusion is active as β-Gal, it should exist as a tetramer. Assays of samples from the induced λ*mycRϕlacZ* lysogen revealed that 450 Miller units of β-Gal activity accumulated before lysis. Assuming a normal specific activity for the mycR–β-Gal fusion protein, this corresponds to approximately 500 molecules of mycR–β-Gal tetramers per cell (see Materials and Methods). Although the number of R molecules produced during the vegetative cycle is not known, previous labeling experiments have suggested that the R protein is produced at levels about equal to those of the S protein (E. Altman and R. Young, unpublished data). Quantitative immunoblotting has been used to estimate S protein levels at about 1,000 to 3,000 molecules per cell at the time of lysis (4). Thus, the level of β-Gal activity is consistent with the estimated number of endolysin molecules and with the notion that the bulk of the hybrid protein is properly folded, active, and tetrameric. Gel filtration chromatography confirmed that the c-*myc* epitope in the mycR–β-Gal fusion protein was present exclusively in size fractions consistent with the tetrameric state (Fig. 4D).

These results demonstrate that the *mycRϕlacZ* gene product is assembled in enzymatically active tetrameric oligomers.

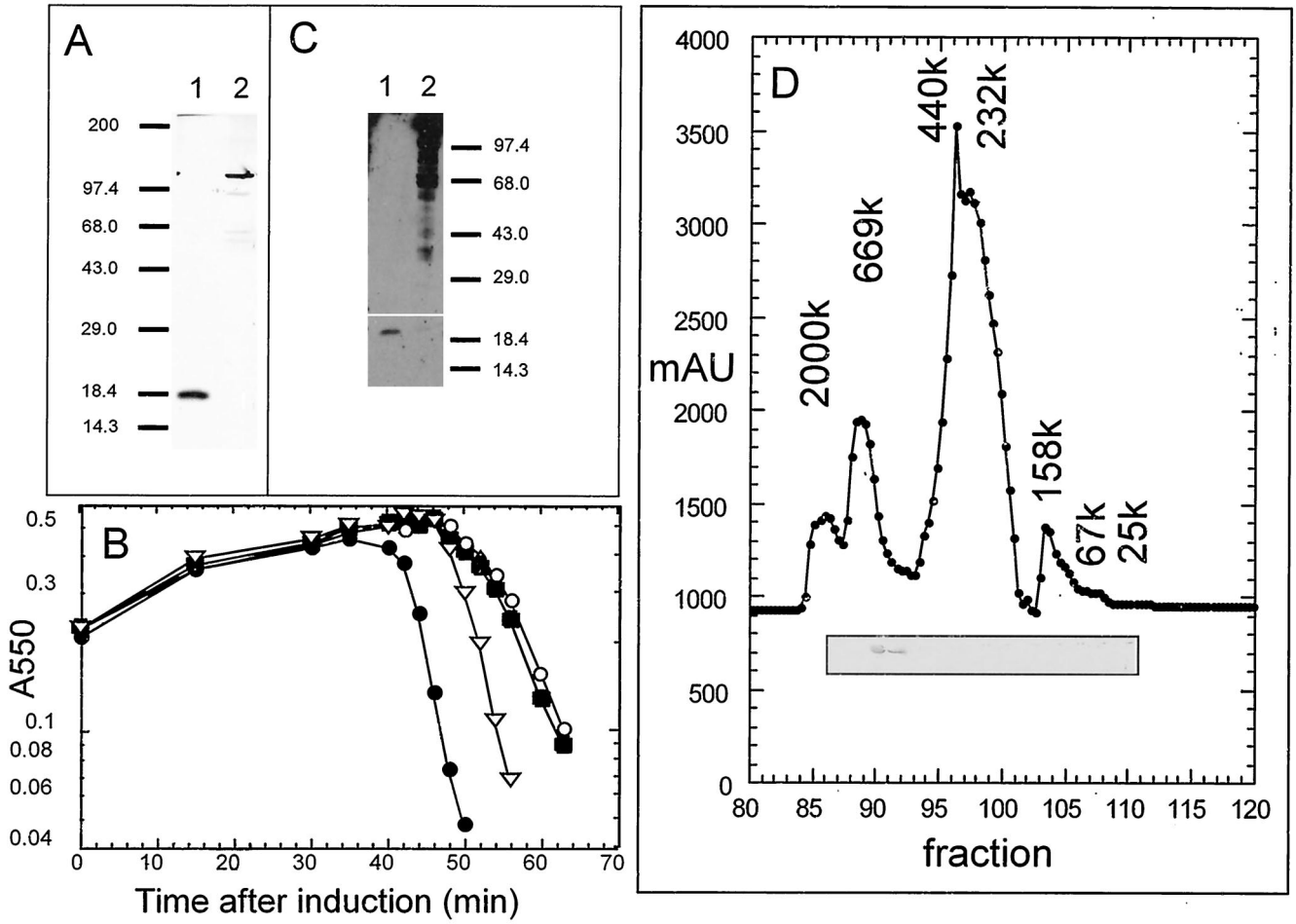

FIG. 4. The lytic function of the hybrid mycR–β-Gal hybrid is not due to proteolytic release of the N-terminal endolysin domain. (A) Full-length mycR and mycR–β-Gal proteins accumulate to equivalent levels. Lysates from the induction of λΔ(*SR*) lysogens carrying pS105mycR (lane 1) or pS105mycRϕlacZ (lane 2) were analyzed by immunoblotting with anti-c-*myc* antibodies. Values at the left are molecular mass standards (in kilodaltons). (B) The level of mycR endolysin is limiting for the rate of lysis. Culture growth and lysis were monitored by determining the A_{550} after the induction of λΔ(*SR*) lysogens carrying pS105mycR (filled circles) or pS105mycRϕlacZ (filled squares). Isogenic lysogens carrying pS105R$^-$ and the compatible plasmid pZS*32-mycR were subjected to lysogenic induction and the addition of either no IPTG (open circles) or 1 mM IPTG (open triangles) at time zero. (C) The levels of R-length proteolytic fragments of the mycR–β-Gal protein were negligible compared to lysis-limiting levels of MycR. Lysates from the induced lysogens carrying pS105mycRϕlacZ or pS105R$^-$ and pZS*32-mycR (no IPTG) were analyzed as described for panel A, except that the stain was deliberately overdeveloped. Values at the right are molecular mass standards (in kilodaltons). (D) Gel filtration chromatography of the mycR and mycR–β-Gal proteins. A lysate prepared from induction of λΔ(*SR*)pS105mycRϕlacZ was analyzed by gel filtration, followed by SDS-PAGE and immunoblotting with anti-c-*myc* antibodies. Shown is the elution pattern for mass standards as indicated, with the blot being superimposed under the appropriate samples. MAU, mass arbitrary units.

Moreover, no R-sized proteolytic fragments were observed, so the lysis supported by this allele was not due to the escape of small N-terminal endolysin domains. We conclude that the S holin-mediated lesion must be sufficiently large to allow efficient release of a roughly globular tetrameric protein of nearly 500 kDa to the peptidoglycan.

Difference between prematurely triggered and early-lysis holin-mediated lesions. Many *S* missense alleles exhibit altered lysis timing, including the early lysis mutant S_{a52g}, which causes lysis at about 10-fold lower levels of S protein than with the parental allele (11). Conceivably, a significant reduction in the number of S proteins might result in significantly smaller lesions and thus restrict the ability of the chimeric mycR–β-Gal endolysin to escape the cytoplasm. To test this idea, isogenic strains were constructed with the early lysis S_{a52g} allele and the *mycR* and *mycRϕlacZ* endolysin alleles; the results show that, despite the reduced total amount of S holin produced by the early lysis allele, the very early S-mediated lesion supported lysis with both the mycR and mycR–β-Gal hybrid endolysins, indicating that the disparity in size between the endolysins did not seriously affect passage across the membrane barrier (Fig. 5A). Early lysis can also be achieved by exogenously imposed depolarization of the membrane during the period when holin protein accumulates in the membrane. Interestingly, premature lysis triggered by cyanide is efficient with the *mycR* allele but not with *mycRϕlacZ* (Fig. 5B and C). This indicates that the membrane lesions formed artificially by prematurely collapsing the membrane potential were smaller than those formed early but spontaneously, with comparable amounts of holin protein, by the missense early-lysis allele. Given the lack

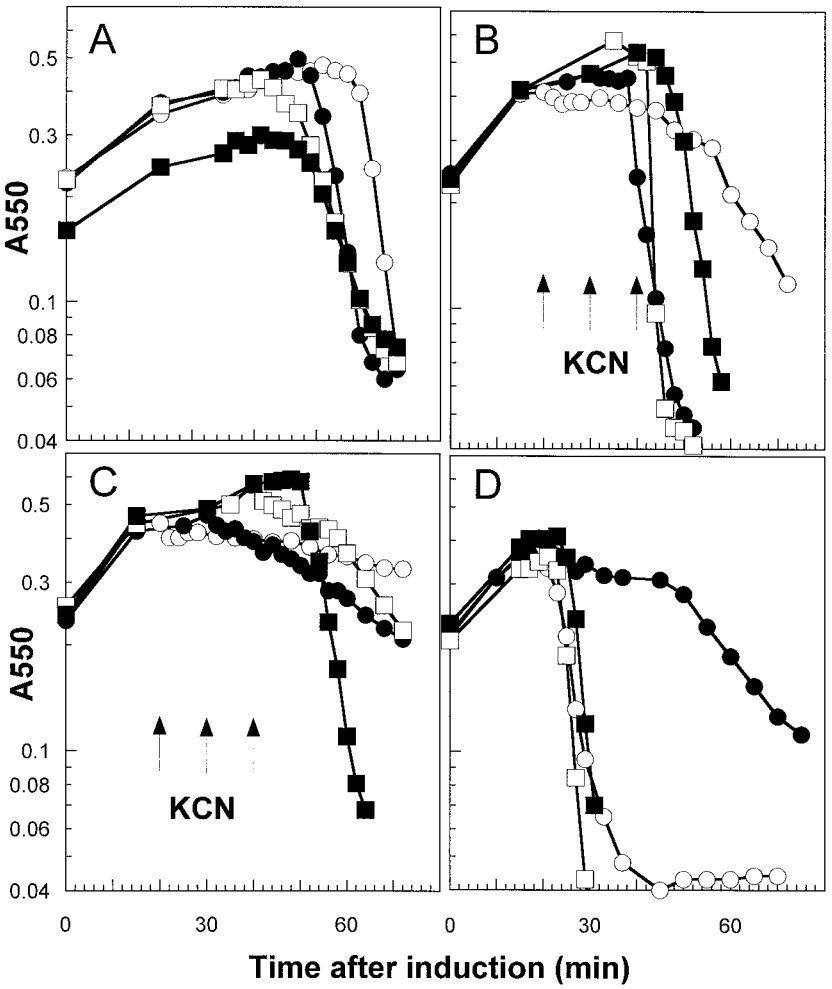

FIG. 5. Abnormal holin lesions can discriminate between the endolysin and the endolysin–β-Gal hybrid. (A) The early-lysis allele of λ *S* supports lysis with both *R* and *RϕlacZ*. Culture growth and lysis were monitored by determining the A_{550} after induction of λΔ(*SR*) lysogens carrying pS105R$^-$ (circles) or pS105A52GR$^-$ (squares). The lysogens also carried a compatible plasmid carrying pZA32-mycR (open symbols) or pZA32-mycRϕlacZ (filled symbols). IPTG (1 mM) was added at the time of lysogenic induction (time zero). (B and C) S holin lesions prematurely triggered by energy poisons are differentially permissive for the mycR and mycR–β-Gal endolysins. Culture growth and lysis were monitored by determining the A_{550} after induction of the λ*S105mycR* (B) or λ*S105mycRϕlacZ* (C) lysogen. KCN (10 mM) was added at 20 min (open circles), 30 min (filled circles) or 40 min (open squares). Filled squares, untreated culture. (D) The parental T4 *t*, but not a *t* allele with its 69 C-terminal residues deleted, supports lysis with both *cmycR* and *cmycRϕlacZ*. Conditions were the same as described for panel A except that the plasmid was pT4-t (squares) or pT4-tΔ69 (circles).

of N-terminal fragments detectable by immunoblotting (Fig. 4C), the gradual cell lysis that was observed in the prematurely triggered inductions with the chimeric endolysin may reflect a small fraction of holes that are sufficiently large to allow the escape of the hybrid protein.

T4 *t*, but not a *t* deletion allele, is permissive for the hybrid endolysin. We wondered if the ability of λ *S* to support the lytic activity of mycR–β-Gal was shared by the other well-studied holin gene, T4 *t*. To answer this question, *t* was cloned under the control of the λ late gene promoter on a medium-copy-number plasmid in *trans* to an inducible Δ*SR* prophage and a compatible plasmid carrying the *mycR* endolysin gene or the *mycRϕlacZ* hybrid endolysin gene under an IPTG-inducible promoter. Induction of the prophage and the endolysin plasmid revealed that the T holin supported a sharply defined lysis event with both the endolysin and endolysin–β-Gal fusion (Fig. 5D). Thus, the T holin, like the S holin, appears to generate a large nonspecific lesion in the membrane. Interestingly, a *t* allele that had inadvertently been generated with a C-terminal deletion was, although supporting lysis with *mycR*, incompetent for lysis with the *mycRϕlacZ* allele (Fig. 5D), suggesting that the lesions generated by the deletion protein were significantly smaller that those generated by the parental T protein.

DISCUSSION

For dsDNA phages, holin-endolysin lysis appears to be the universal solution to the critical problem of how to achieve efficient and appropriately scheduled host lysis. The roles of the two proteins are clearly defined in the lysis system of phage λ. The R endolysin destroys the murein; the S holin controls the function of the endolysin by forming a lethal membrane lesion at a precisely scheduled time. In several other bacteriophages (e.g., T4, P22, and T7), the formation of the holin

lesion permits escape of the endolysin from the cell (27, 31); in other cases, where the endolysin achieves export by the secretory machinery, the formation of the holin lesion collapses the membrane potential and apparently activates the endolysin (20) (M. Xu, I.-N. Wang, and R. Young, unpublished data). The specificity, enzymatic activity, and tertiary structure of a number of prototype endolysins are well understood (5, 6, 28); however, the nature of the holin-mediated membrane lesion is still not known for any of the holins.

Sizing the S-mediated lesion. Here we have shown that the membrane lesion effected by the λ S holin is capable of allowing release of the product of a *Rϕlac*Z fusion gene containing all of the codons of both *R* and *lacZ*. The hybrid is an active β-Gal tetramer with a mass in excess of 480 kDa, about 30-fold greater than the 18 kDa of the parental R endolysin. To accomplish efficient release of the hybrid mycR–β-Gal, the holin-mediated lesion would have to be much larger than any characterized transmembrane channel formed from intracellular components. For example, the putative SecYEG translocon channel, estimated to have an internal diameter of 1.5 to 2 nm from transmission electron microscope studies, effects the translocation of unfolded polypeptides (13). The membrane machinery of the TAT pathway for export of partially folded, coenzyme-liganded periplasmic proteins appears to have a central chamber about 6 nm in diameter (21), but it is highly specific for proteins carrying the TAT signal and is carefully gated. The only membrane channels of comparable size are the 30-nm-diameter cytocidal β-sheet channels formed in mammalian membranes by the streptolysin-O class of thiol-activated cytotoxins (1, 22); however, these toxins are soluble exoproteins that undergo a complex tertiary and quaternary rearrangement once bound to the membrane.

Size and numbers of holes. We cannot rule out the possibility that the small but reproducible delay in lysis observed with spontaneous triggering, but not with chloroform treatment, of the cells producing the endolysin–β-Gal hybrid might reflect some restriction on the passage of the larger chimeric endolysin through the spontanous holes, slower diffusion within the periplasm from the points of spontaneous membrane disruption, or reduced enzymatic activity of the chimera with the murein substrate. Presumably, neither of these substrate access defects would be observed in the case of general permeabilization with chloroform. Moreover, even a substantial reduction in catalytic efficiency might not be detectable in whole-cell lysis profiles, so the data presented here do not support the conclusion that the chimeric endolysin is exactly equivalent to the normal-sized enzyme either in accessing the murein or in degrading it once it is localized in the periplasm. Nevertheless, a proteinaceous hole with a diameter sufficient for the escape of the full-sized chimera would be of a size unprecedented for protein channels formed in a cell membrane, irrespective of the altered kinetic characteristics of the hybrid protein.

Implications for holin function and timing. These findings significantly constrain models for holin timing and function. With cytolytic toxins and the complement-perforin systems, the membrane lesion is assembled from extracellular soluble components that polymerize at the external membrane surface and undergo massive conformational changes as they become inserted in the membrane (23). Membrane damage is progressive as each subunit penetrates the bilayer. In contrast, biochemical and physical data show that the S protein appears to have three unremarkable alpha-helical TMDs. It is difficult to imagine that the S molecule undergoes significant topological change, given its predominantly alpha-helical structure and common oligotopic disposition in the membrane. There is virtually no precedent for a helical transmembrane domain, once stably incorporated into the membrane, to change to another secondary structure or exit the membrane entirely. It is much more likely that the molecular basis of hole formation is a tertiary rearrangement of the helices within the S protein and a quaternary rearrangement of S molecules. Heretofore, holin-mediated lesions have been considered to be proteinaceous pores of some size. The remarkable size tolerance of the S-mediated lesion suggests an alternative perspective in which the holins cause a radical, if localized, disruption of the membrane, rather than a regular proteinaceous channel.

Given the small size of the S holin and other holins, it is difficult to avoid the requirement that the S molecules form large two-dimensional aggregates in the membrane, or patches, prior to triggering. A model incorporating this fundamental notion is shown in Fig. 6. According to this idea, the holins first dimerize and then accumulate in higher-order oligomers which coalesce into rafts, largely excluding lipid from the interior. Early in raft formation, the forces determining the stability of the aggregate are dominated by lipid-protein interactions; as the rafts increase in size, protein-protein interactions, presumably mostly defined by intermolecular helical packing, begin to dominate. This model allows all of the surfaces of the transmembrane domains to be involved in the oligomerization process, consistent with the findings that conservative changes in all three TMDs have drastic effects on lysis timing, both accelerating and retarding the "lysis clock" (7). The idea is that, at some point in the growth of the patch, thermal fluctuation opens a momentary channel or hole in the protein array. The S holin triggers hole formation when the cellular proton motive force is reduced by about 40% (9), so it is expected that this instantaneous local depolarization of the membrane would in turn catalyze conformational changes that further weaken the protein-protein interactions of at least some of the surfaces of the holin, leading to further spreading of the depolarization wave and thus rapidly to much larger holes or lesions in the membrane (Fig. 6A).

This type of model is attractive because it does not require any particular structure for the holin molecules other than having TMDs that can support intimate helix-helix packing. The unprecedented diversity of holins makes it hard to imagine how regular proteinaceous pores could be assembled from all of them. It also helps to account for the marked sensitivity of the TMDs of the S protein to changes in side chains; small changes at many different positions lead to dramatic effects on lysis timing (7, 8, 16). These large changes in the triggering time may reflect changes in the strength of interactions leading to patch formation or maintenance of patch integrity. Furthermore, the model may explain the existence not only of partially dominant and recessive *S* lysis-defective alleles but also of the unexpected class of "antidominant" lysis-defective alleles, which lead to early lysis in the presence of the wild type (27). A side chain alteration which, as a result of the consequent defect in the packing of the helical TMDs, blocks some step in

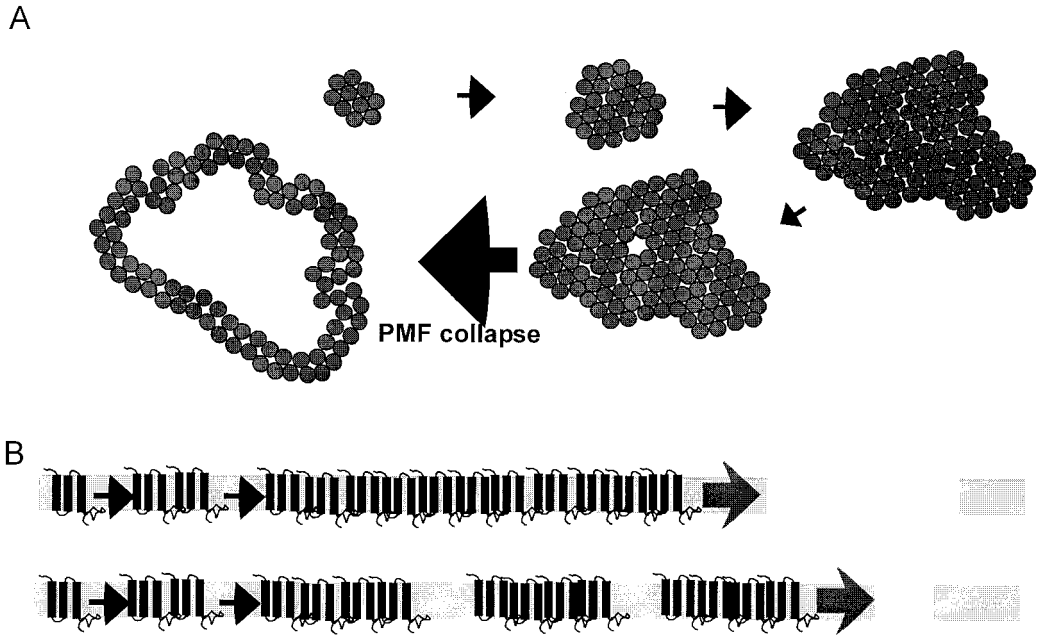

FIG. 6. Model for the formation of a holin lesion. (A) Holin rafts. Holins accumulate in rafts in the membrane; intimate helix packing by TMDs largely excludes lipids. Each circle represents a single holin molecule. Spontaneous formation of an aqueous channel by thermal fluctuation is depicted. The localized depolarization causes a conformational change in the holins, leading to asymmetric disruption of the helix packing, exposure of a relatively hydrophilic surface, and dispersion of the subunits into the holin lesion. PMF, proton motive force. (B) Hole size. A schematic representation of the formation of large lesions by the wild-type holin and smaller lesions by a mutant that accretes into more numerous, but smaller, rafts.

oligomerization or the quaternary rearrangement in the homo-oligomeric case may facilitate either process in hetero-oligomers with the wild-type holin. Lysis-defective *S* mutants which are blocked in dimerization and oligomerization are known, and the model predicts them to abolish raft formation. Moreover, many lysis-defective mutants are blocked in an oligomerized state (8) and all of these alleles lack the ability to be triggered by energy poisons like cyanide. We suggest that these mutants are defective in the last step of the proposed pathway and are unable to propagate the wave of depolarization throughout the raft of S molecules. The selectivity of the partially defective T protein can also be rationalized with this model. Presumably, the altered T protein, when it triggers, simply does not form sufficiently large protein-bounded lesions and thus can function to release the normal-sized 18-kDa endolysin but not the bigger chimeric endolysin molecule (Fig. 6B).

In these experiments, the lesions mediated by the early-lysis S_{a52g} allele are permissive for the endolysin–β-Gal hybrid but not for the lesions prematurely triggered by cyanide. This finding suggests that there is a relationship between spontaneous triggering and the size of the holin-mediated lesion. The simplest notion is that the size of the raft of holin molecules is related to the spontaneous triggering time. The early-lysis alleles, which do not result in higher rates of holin accumulation (11), may generate larger-than-average rafts earlier after induction of the holin gene. Thus, premature triggering by an energy poison would result in a smaller lesion, irrespective of the allelic state of the holin gene, within certain limits. Alternatively, or additionally, the final average depth of the lining at the edges, in terms of layers of holin molecules, may also be related to how the triggering occurs.

We have previously shown, using alleles of the holin genes *S* and *T*, that there is a synergistic effect of having the two unrelated holins accumulating in the membrane; that is, the onset of lysis occurs significantly earlier with both holins being produced than with either holin alone (17). One possibility, of course, is that the two holins, despite their disparate origins and lack of relatedness at the sequence and topological levels, somehow form a common mass action pool. It seems unlikely that the TMDs of the two holins engage in productive helical packing, especially considering the dramatic sensitivity of both the S and T holins to subtle changes in side chains within the TMDs (8, 18). However, the model presented here suggests that the answer may lie in what drives the formation of the holin rafts. We suggest that the driving force for the sequestering of these proteins, even at low concentrations within the membrane, is a relatively lipophobic character in one or more of the TMDs of the holins. Thus, the holin is forced into the membrane by the insertion machinery of the host but then aggregates to minimize the exposure to the lipid environment of the bilayer. Thus, mixed rafts consisting of minirafts of the different holins might easily form during the induction of the heterologous holin genes. The effect would be to have a larger pool of holins accumulating and thus could account for the unexpected early lysis in the coexpression constructs.

The model makes a clear prediction that the holins will be found in rafts in the membrane. If biochemical and cytological evidence for patch formation can be obtained, the next chal-

lenge would be to develop a quantitative model rationalizing how the two-dimensional patch model can account for the precise lysis timing required for holin function.

ACKNOWLEDGMENTS

We thank the members of the Young laboratory, who provided much assistance and critical input. Norma Teetes provided essential clerical help.

This work was supported by funds from the Public Health Service (grant NIGMS 27099), the Robert A. Welch Foundation, and the Texas Agricultural Experiment Station.

REFERENCES

1. **Bhakdi, S., J. Tranum-Jensen, and A. Sziegoleit.** 1985. Mechanism of membrane damage by streptolysin-O. Infect. Immun. **47:**52–60.
2. **Bläsi, U., P. Fraisl, C.-Y. Chang, N. Zhang, and R. Young.** 1999. The C-terminal sequence of the ë holin constitutes a cytoplasmic regulatory domain. J. Bacteriol. **181:**2922–2929.
3. **Bläsi, U., K. Nam, D. Hartz, L. Gold, and R. Young.** 1989. Dual translational initiation sites control function of the lambda *S* gene. EMBO J. **8:**3501–3510.
4. **Chang, C.-Y., K. Nam, and R. Young.** 1995. *S* gene expression and the timing of lysis by bacteriophage λ. J. Bacteriol. **177:**3283–3294.
5. **Cheng, X., X. Zhang, J. W. Pflugrath, and F. W. Studier.** 1994. The structure of bacteriophage T7 lysozyme, a zinc amidase and an inhibitor of T7 RNA polymerase. Proc. Natl. Acad. Sci. USA **91:**4034–4038.
6. **Evrard, C., J. Fastrez, and J. P. Declercq.** 1998. Crystal structure of the lysozyme from bacteriophage lambda and its relationship with V and C-type lysozymes. J. Mol. Biol. **276:**151–164.
7. **Gründling, A., U. Bläsi, and R. Young.** 2000. Biochemical and genetic evidence for three transmembrane domains in the class I holin, λ S. J. Biol. Chem. **275:**769–776.
8. **Gründling, A., U. Bläsi, and R. Young.** 2000. Genetic and biochemical analysis of dimer and oligomer interactions of the λ S holin. J. Bacteriol. **182:**6082–6090.
9. **Gründling, A., M. D. Manson, and R. Young.** 2001. Holins kill without warning. Proc. Natl. Acad. Sci. USA **98:**9348–9352.
10. **Jacobson, R. H., X. J. Zhang, R. F. DuBose, and B. W. Matthews.** 1994. Three-dimensional structure of β-galactosidase from *E. coli*. Nature **369:**761–766.
11. **Johnson-Boaz, R., C.-Y. Chang, and R. Young.** 1994. A dominant mutation in the bacteriophage lambda *S* gene causes premature lysis and an absolute defective plating phenotype. Mol. Microbiol. **13:**495–504.
12. **Lutz, R., and H. Bujard.** 1997. Independent and tight regulation of transcriptional units in *Escherichia coli* via the LacR/O, the TetR/O and AraC/I1-I2 regulatory elements. Nucleic Acids Res. **25:**1203–1210.
13. **Meyer, T. H., J. F. Menetret, R. Breitling, K. R. Miller, C. W. Akey, and T. A. Rapoport.** 1999. The bacterial SecY/E translocation complex forms channel-like structures similar to those of the eukaryotic Sec61p complex. J. Mol. Biol. **285:**1789–1800.
14. **Miller, J. H.** 1972. Experiments in molecular genetics. Cold Spring Harbor Laboratory, Cold Spring Harbor, N.Y.
15. **Phillips, A. T.** 1994. Enzymatic activity, p. 555–586. *In* P. Gerhardt, R. G. E. Murray, W. A. Wood, and N. R. Krieg (ed.), Methods for general and molecular bacteriology. ASM Press, Washington, D.C.
16. **Raab, R., G. Neal, C. Sohaskey, J. Smith, and R. Young.** 1988. Dominance in lambda *S* mutations and evidence for translational control. J. Mol. Biol. **199:**95–105.
17. **Ramanculov, E. R., and R. Young.** 2001. Functional analysis of the T4 *t* holin in a lambda context. Mol. Genet. Genomics **265:**345–353.
18. **Ramanculov, E. R., and R. Young.** 2001. Genetic analysis of the T4 holin: timing and topology. Gene **265:**25–36.
19. **Rietsch, A., P. Fraisl, A. Graschopf, and U. Bläsi.** 1997. The hydrophilic C-terminal part of the lambda S holin is non-essential for intermolecular interactions. FEMS Microbiol. Lett. **153:**393–398.
20. **São-José, C., R. Parreira, G. Vieira, and M. A. Santos.** 2000. The N-terminal region of the *Oenococcus oeni* bacteriophage fOg44 lysin behaves as a bona fide signal peptide in *Escherichia coli* and as a *cis*-inhibitory element, preventing lytic activity on oenococcal cells. J. Bacteriol. **182:**5823–5831.
21. **Sargent, F., U. Gohlke, E. de Leeuw, N. R. Stanley, T. Palmer, H. R. Saibil, and B. C. Berks.** 2001. Purified components of the Escherichia coli Tat protein transport system form a double-layered ring structure. Eur. J. Biochem. **268:**3361–3367.
22. **Sekiya, K., H. Danbara, K. Yase, and Y. Futaesaku.** 1996. Electron microscopic evaluation of a two-step theory of pore formation by streptolysin O. J. Bacteriol. **178:**6998–7002.
23. **Shatursky, O., A. P. Heuck, L. A. Shepard, J. Rossjohn, M. W. Parker, A. E. Johnson, and R. K. Tweten.** 1999. The mechanism of membrane insertion for a cholesterol-dependent cytolysin: a novel paradigm for pore-forming toxins. Cell **99:**293–299.
24. **Smith, D. L., C.-Y. Chang, and R. Young.** 1998. The λ holin accumulates beyond the lethal triggering concentration under hyper-expression conditions. Gene Expr. **7:**39–52.
25. **Smith, D. L., D. K. Struck, J. M. Scholtz, and R. Young.** 1998. Purification and biochemical characterization of the lambda holin. J. Bacteriol. **180:**2531–2540.
26. **Smith, D. L., and R. Young.** 1998. Oligohistidine tag mutagenesis of the ë holin gene. J. Bacteriol. **180:**4199–4211.
27. **Wang, I.-N., D. L. Smith, and R. Young.** 2000. Holins: the protein clocks of bacteriophage infections. Annu. Rev. Microbiol. **54:**799–825.
28. **Weaver, L. H., and B. W. Matthews.** 1987. Structure of bacteriophage T4 lysozyme refined at 1.7 Å resolution. J. Mol. Biol. **193:**189–199.
29. **Wessel, D., and U. I. Flügge.** 1984. A method for the quantitative recovery of protein in dilute solution in the presence of detergents and lipids. Anal. Biochem. **138:**141–143.
30. **Wu, L. F., B. Ize, A. Chanal, Y. Quentin, and G. Fichant.** 2000. Bacterial twin-arginine signal peptide-dependent protein translocation pathway: evolution and mechanism. J. Mol. Microbiol. Biotechnol. **2:**179–189.
31. **Young, R., I.-N. Wang, and W. D. Roof.** 2000. Phages will out: strategies of host cell lysis. Trends Microbiol. **8:**120–128.